# Theoretical Study of Toluene Chemisorption on Si(100)

**Francesca Costanzo,[†] Carlo Sbraccia,[†,‡] Pier Luigi Silvestrelli,*[,†] and Francesco Ancilotto[†]**

*Udr Padova, INFM, via Marzolo 8, I-35131 Padova, Italy, DEMOCRITOS National Simulation Center, INFM, via Beirut 2/4, 34014 Trieste, Italy, Dipartimento di Fisica "G. Galilei", Università di Padova, via Marzolo 8, I-35131 Padova, Italy, and Scuola Internazionale Superiore di Studi Avanzati (SISSA), via Beirut 2/4, 34014 Trieste, Italy*

*Received: April 14, 2003; In Final Form: June 12, 2003*

The chemisorption of toluene on the Si(100) surface is studied using first principles and semiempirical methods. We find that the most stable configuration is a dissociated one, in which a C−H bond of the methyl group is cleaved and the loose hydrogen is bonded to the silicon surface; a detailed analysis based on the use of the maximally localized Wannier functions indicates that this process can be described as a proton abstraction reaction. Several other stable geometries involving both undissociated and dissociated toluene molecules have been found and studied. Although most of them resemble those of benzene on Si(100), some differences have been detected, which mainly reflect the role of the electron-donating, substituent methyl group of toluene. Possible reaction pathways leading from one stable adsorption configuration to another and to the dissociation of the toluene molecule on the Si surface have been investigated; in particular the one involving the abstraction of a proton from the methyl group has been found to be activated, with an energy barrier of about 1.4 eV. Our results are compared with recent experimental measurements.

## I. Introduction

Surface phenomena have always been a cornerstone of the microelectronics industry. Processes such as epitaxy[1] and chemical vapor deposition, etching, oxidation, and passivation,[2] which are used routinely in the industry, involve chemical or physical processes occurring at the surface of the semiconductor wafer. Understanding of the atomic-level phenomena underlying these processes becomes more and more critical. As a result, the importance of atomic-level surface chemistry is highlighted in the growing field of organic functionalization of semiconductors. In particular, the Si(100) surface has become one of the most important substrates for the microelectronics industry because of its special structural and electronic properties. This reactive surface consists of rows of buckled surface dimers which can be described as having both $\pi$ bond character and zwitterionic diradical character, with the lower Si atom of the buckled pair characterized by a partial positive charge and the upper atom by a partial negative charge. This dual nature allows the Si(100) surface dimers to act as both double bonds and electrophilic/nucleophilic moieties, and is responsible for the steadily increasing number of types of reactions used to bind organic molecules onto this surface. The adsorption of unsaturated aromatic hydrocarbons on the Si(100) surface is a topic of great current interest[3,4] both because it represents a prototype system for the study of molecular adsorption (and desorption) of hydrocarbons on semiconductor surfaces and also because it is considered a promising precursor of technologically relevant processes, such as the chemical vapor deposition of diamond thin films on Si surfaces and the growth of silicon carbide (SiC).[5]

Toluene ($C_7H_8$) and benzene ($C_6H_6$) are the most important unsaturated aromatic hydrocarbons in organic chemistry. The adsorption of benzene on the Si(100) surface has been intensively examined in recent years. On the basis of a combined study using high-resolution electron-energy-loss spectroscopy (HREELS), thermal desorption spectroscopy (TDS), and Auger electron spectroscopy (AES), Taguchi et al.[6] showed that benzene chemisorbs molecularly on Si(100) at room temperature, and thus proposed that benzene is di-$\sigma$-bonded to two Si atoms of a dimer on the surface. Scanning tunneling microscopy (STM) studies at room temperature by Lopinski et al.[7] have revealed the presence of multiple configurations, which were identified as on top of a single dimer and two different bridging geometries involving two dimers. In addition, the STM experiments identified a single-dimer geometry as a metastable precursor to the bridging configurations involving two adjacent Si surface dimers. Using ab initio calculations, Wolkow et al.[8] associated the single-dimer configuration with a 1,4-cyclohexadiene-like structure that was di-$\sigma$-bonded to a single surface Si dimer, and the two different double-dimer geometries with a "tight bridge" (TiB) configuration and with a C-type-defect "twisted bridge" (TwB) configuration,[9] respectively. The results of multiple internal reflection Fourier transform infrared (MIR-FTIR) spectroscopy and near-edge X-ray absorption fine structure (NEXAFS) studies of chemisorbed benzene at 100 K and at room temperature were consistent with those of benzene forming a 1,4-cyclohexadiene-like structure.[10] Recent first principles theoretical calculations of adsorption of benzene on the Si(100) surface[11] have revealed that the most stable configuration is a tetra-$\sigma$-bonded structure characterized by one C−C double bond and four C−Si bonds. However, according to the results of ref 11, a benzene molecule impinging on the Si surface is most likely to be adsorbed in one of three different, metastable di-$\sigma$-bonded structures, characterized by two C−Si bonds, and eventually converts into the lowest-energy configurations.

The study of adsorption of toluene on silicon surfaces represents a natural extension of the case of benzene. In

[†] INFM and Università di Padova.
[‡] SISSA.
* Corresponding author.

10.1021/jp0349987 CCC: $25.00 
Published on Web 08/22/2003

particular, it would be interesting to understand how the presence of the methyl group ($CH_3$) alters the peculiar properties of benzene on the Si(100) surface. It is well-known that substituent groups on an aromatic ring may steer the ring into particular bonding configurations on the Si surface.[12] Recently, Borovsky et al.[13] reported an STM study on the adsorption of toluene on Si(100), which suggests that room temperature adsorption occurs on top of the Si dimer rows, giving rise to several binding geometries that closely resemble those of benzene on the same surface. They also found that toluene decomposes at elevated temperatures, leaving carbon on the surface, eventually leading to the formation of small SiC clusters. At variance with the case of benzene, however, one of the structures observed with STM suggests that toluene may interact with more than two adjacent Si dimers. Recent work of Coulter et al.,[12] based on Fourier transform infrared (FTIR) spectroscopy, shows that the methyl-substituted aromatic hydrocarbons are chemisorbed on Si(100) in multiple configurations, in much the same way as benzene. These authors suggest that dissociation occurs after chemisorption through the cleavage of a C−H bond of the substituent methyl group, leaving the carbon ring intact. In fact peaks in the Si−H stretching region were observed in the FTIR spectra, indicating some dissociation of methyl-substituted molecules upon adsorption, with the subsequent sticking of the detached H atom to a clean Si dimer. Li and Leung,[14] using thermal desorption spectroscopy (TDS), low-energy electron diffraction (LEED), and AES, confirmed the results of Coulter et al.; in particular their TDS study showed three molecular desorption features, at 350, 430, and 530 K, which were assigned (see Table 1 in ref 14) to defect sites ($\alpha$ state), adsorption configurations involving a single Si dimer of the (100) surface ($\beta$ state), and adsorption configurations involving two surface Si dimers ($\gamma$ state). According to Li and Leung,[14] these observed desorption maxima remain essentially unchanged with increasing exposure, indicating first-order desorption kinetics. They suggested that only toluene in the double-dimer adsorption configuration ($\gamma$ state) undergoes molecular desorption, while toluene molecules in the $\alpha$ and $\beta$ states, at room temperature (RT), readily lose the benzylic hydrogen, allowing for the methylene group to bind to a neighboring dimer on the Si surface. Starting from the consideration that benzene and toluene show very similar desorption maxima and first-order desorption kinetics, Li and Leung[14] conclude that RT adsorption of toluene involves binding arrangements similar to those of benzene. One significant difference between the adsorption of benzene and toluene on Si(100) is that the desorption intensity of toluene is considerably weaker than that of benzene for the same RT exposure. Moreover, by means of AES measurements, Li and Leung[14] determined the saturation coverage for toluene to be 0.33 monolayer (ML). The difference with respect to the saturation coverage of benzene, found by Taguchi et al.[6] to be 0.27 ML, could suggest that the weak molecular desorption observed for toluene is not due to lower coverage but rather to possible reactions that reduce the toluene concentration. In addition, the higher saturation coverage for toluene relative to benzene indicates a stronger adsorbate−substrate interaction than adsorbate−adsorbate interaction. To provide new insights into the interactions of unsaturated cyclic hydrocarbons on Si(100) and to help the interpretation of experimental results, we have studied chemisorption of toluene on the Si(100) surface using both a first principles approach and a semiempirical approach.

## II. Method

First principles calculations have been carried out within the *Car−Parrinello* approach[15] in the framework of density functional theory (DFT), using gradient corrections in the PBE implementation.[16] Gradient-corrected functionals have been adopted in the most recent theoretical studies of adsorption of organic molecules on Si(100) because they are typically more accurate than the simple local density functional in describing chemical processes on this surface.[17,18] In particular we adopted the PBE functional, because of its strong physical background and its reliability in a number of studied systems. Although most of our calculations have been performed by adopting a spin-restricted approach, additional tests have been carried out, using instead a spin-unrestricted scheme, in cases where unpaired electrons are expected to play a possible role: no significant differences have been found. The calculations have been carried out considering the $\Gamma$ point only in the Brillouin zone (BZ), and using norm-conserving pseudopotentials,[19] with s and p nonlocality for C and Si. Wave functions were expanded in plane waves with an energy cutoff of 50 Ry. We have explicitly checked that, at this value of the energy cutoff, the structural and binding properties of our system are well converged. We used a slab model to simulate the Si surface in the $2 \times 2$ reconstruction. The slab is made of five Si layers, plus a vacuum region, 6 Å wide, separating the repeated images of the slab. A monolayer of hydrogen atoms is used to saturate the dangling bonds on the lower surface of the slab. We have used a supercell with a $p(\sqrt{8}\times\sqrt{8})R45°$ periodicity, i.e., with four Si surface dimers. On the basis of previous experience in simulations of similar systems,[11,20,21] we expect that, with such a supercell, a sampling of the BZ limited to the $\Gamma$ point is adequate. We verified that, by starting with the unreconstructed, clean Si(100) surface, the structural optimization procedure correctly produces asymmetric surface dimers, with a dimer bond length and buckling angle in good agreement with previous, highly converged ab initio calculations.[22] Structural relaxations of the ionic coordinates have been performed using the method of direct inversion in the iterative subspace.[23] A different, larger supercell characterized by a $p(4\times4)$ periodicity, containing a slab of 6 Si layers (with 16 atoms for each layer, i.e., 8 Si surface dimers), has been used to check for finite-size effects and/or different surface coverages, as explained in the following. During the ionic relaxations and molecular dynamics (MD) simulations, the lowest Si layer and the saturation hydrogens were kept fixed to the bulk crystallographic positions. To better investigate the complex potential energy surface of this system, in some cases the optimization procedure was repeated using a simulated-annealing strategy and starting from different initial configurations.

An extensive set of preliminary calculations have been performed using semiempirical potentials within classical MD calculations. This allowed us to rapidly explore a larger portion of the configurational space to search efficiently for stable chemisorbed structures, possible dissociation pathways, and dissociation products; then the resulting structures and pathways were reinvestigated, using the more accurate ab initio approach described above. We find this procedure particularly effective in systems such as the one studied here, where a large number of possible structures and bonding geometries are possible: an already good guess for the structures to be studied allows the results to be found more rapidly and with much less computational effort at the ab initio level.

The semiempirical calculations have been performed using the so-called "extended Brenner potential" (XB potential hereafter), a multiparticle interatomic potential based on the bond-order concept,[24,25] which takes into account the chemical environment of each bond and is able to describe processes

**TABLE 1: Geometry and Vibrational Frequencies of the Free $C_7H_8$ Molecule[a]**

| | calcn | expt | | calcn | expt |
|---|---|---|---|---|---|
| $C_{ring}$–H (Å) | 1.10 | 1.11 | C−H stretching ($cm^{-1}$) | 3185 | 3005 |
| $C_{ring}$–$C_{ring}$ (Å) | 1.40 | 1.40 | C−C stretching ($cm^{-1}$) | 1609 | 1600 |
| $C_{ring}$–$CH_3$ (Å) | 1.51 | 1.52 | | | |

[a] The results of our calculations are compared with the experimental data.[30]

characterized by bond breaking and/or bond formation. The XB semiempirical potential has been successfully applied to a number of systems and, in particular, used to investigate the chemisorption of $C_2H_2$, $CH_3$, and $Si_2H_6$ on the Si(100) surface.[26,27] Recently an improved parametrization of the XB potential has been proposed[28] to overcome some limitations of the original potential. In particular, the modified potential, based on this new parametrization (mXB for short in the following), allowed a more accurate description of chemisorption energies of aromatic molecules, such as benzene, on the Si(100) surface. For this reason the mXB potential has been employed in the present work.

Accurate estimates of the pathways and energy barriers characterizing the different dissociation processes have been obtained from first principles by means of a recently proposed variant of the popular "nudged elastic band" method, i.e., the "climbing image nudged elastic band"(CI-NEB) method,[29] which has proven to be a very efficient technique to determine minimum energy paths (MEPs) in complex chemical reactions. We estimate that our computed binding energies and energy barriers are affected by an an average error bar of ∼0.1 eV (∼2 kcal/mol), which is the typical accuracy allowed by present-day first principles approaches based on DFT.

## III. Results

As a preliminary test we have calculated, from first principles, the structural and vibrational properties of the free toluene molecule (see Table 1) and found good agreement with the experimental data.[30]

Toluene differs chemically from benzene only by the replacement of a hydrogen atom by a methyl ($CH_3$) group. The methyl group on the aromatic ring can induce the activation of the ortho and para positions of the phenyl ring toward an electrophilic reagent, owing to the electron donator character of the methyl group, characterized by an $sp^3$ orbital nature, toward the $sp^2$ orbitals of C atoms within the ring. These activated C atoms in turn may favorably bind to the Si surface. Aromatic hydrocarbons typically interact with reactants in one of two ways. In *substitution* reactions, a C−H bond on the ring is cleaved as the reactant attacks one of the aromatic carbon atoms; in *addition* reactions, the reactant bonds directly to the ring through the $\pi$ system without cleavage of C−H bonds. For aromatic hydrocarbons, substitution reactions preserve the aromaticity of the benzene ring, while, in addiction reactions, the aromaticity of the ring is lost. Our results show that the toluene dissociation involves almost exclusively the methyl group, not the ring. These observations suggest that the interaction of these aromatic systems with the Si(100) surface more closely mimics addiction reactions, as proposed in ref 12; in particular, binding will be favored to "down" (electrophilic) Si atoms of the surface dimers. Different binding configurations are thus possible, depending on the position of the methyl group with respect to the underlying Si dimers. We have explored systematically these various structures, considering both dissociated and undissociated chemisorbed configurations.

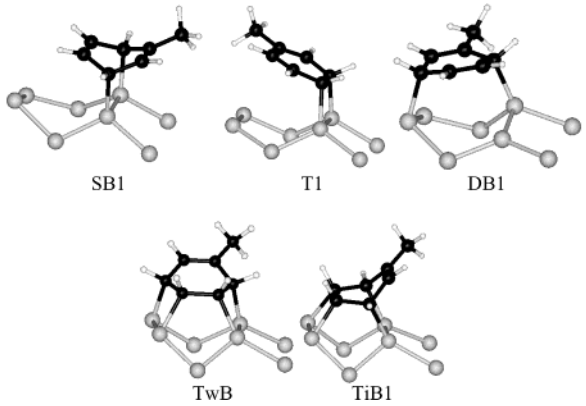


**Figure 1.** Stable undissociated configurations for chemisorption of toluene on Si(100). White, black, and gray balls indicate H, C, and Si atoms, respectively. For clarity only a few surface Si atoms are shown.

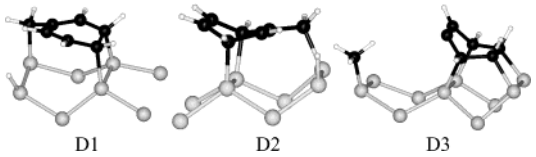


**Figure 2.** Stable dissociated configurations for chemisorption of toluene on Si(100).

**TABLE 2: Binding Energies (eV) of Different Configurations of Toluene (Shown in Figures 1 and 2) Chemisorbed on Si(100) in the 2 × 2 Reconstruction Using the Two Different Supercells[a]**

| config | $p(\sqrt{8}\times\sqrt{8})R45°$ | $p(4\times4)$ | config | $p(\sqrt{8}\times\sqrt{8})R45°$ | $p(4\times4)$ |
|---|---|---|---|---|---|
| TiB1 | 1.11 | 1.49 | T1 | 0.65 | 0.76 |
| TwB | 1.09 | 1.28 | T2 | 0.60 | |
| SB1 | 1.04 | 1.32 | T3 | 0.45 | |
| TiB2 | 0.99 | | D1 | 1.68 | 1.84 |
| TiB3 | 0.95 | | D2 | 2.19 | 2.48 |
| SB2 | 0.88 | | D3 | unstable | 0.66 |
| DB1 | 0.83 | 0.96 | polymer | | 5.72 |

[a] See the text for details. In the case of the larger $p(4\times4)$ supercell only the main configurations have been considered.

The resulting optimized structures are shown in Figures 1 and 2. For clarity we distinguish among the structures involving the intact toluene molecule (Figure 1) and those where dissociation of the molecule occurred (Figure 2). The binding energies of the various configurations are given in Table 2, while the structural parameters are reported in Table 3 (in this case we only give data obtained using the $p(4\times4)$ supercell; the corresponding values obtained with the smaller $p(\sqrt{8}\times\sqrt{8})R45°$ supercell differ only by ±0.01 Å). Given the similarities with the case of benzene, we adopt here the same nomenclature used to describe the various adsorption states of benzene on Si(100).[11] Furthermore, a given adsorbed configuration of the intact molecule is labeled with a number: different numbers indicate different positions of the $CH_3$ group within the ring. For instance, the T structure (which is described in detail below) can occur in three different nonequivalent configurations: T1 (shown in Figure 1), T2, and T3. In the T2 configuration the methyl group is attached to a C atom of the ring next to the C atom bonded to the underlying Si surface atom, whereas in the T3 configuration the methyl group is attached on the C atom which is bonded to the Si surface.

Among the *undissociated* chemisorbed structures, and just like in the case of benzene on Si(100),[11] the TiB and TwB configurations (see Figure 1) have the largest binding energies: they are tetra-$\sigma$-bonded structures characterized by the

**TABLE 3: Bond Lengths (Å) Relative to the Different Studied Configurations, Using the $p(4\times4)$ Supercell[a]**

| config | Si−Si | C−$C_b$ | C−C | C−C | C−C | C−C | C−C | $C_b$−Si |
|---|---|---|---|---|---|---|---|---|
| T | 2.36 | 1.55 | 1.48 | 1.36 | 1.45 | 1.37 | 1.48 | 2.04 |
| SB | 2.39 | 1.36 | 1.50 | 1.50 | 1.36 | 1.51 | 1.50 | 1.98 |
| config | Si−Si | Si−Si | C−$C_b$ | C−C | C−C | C−C | C−C | $C_b$−Si |
| D1 | 2.42 | 2.36 | 1.56 | 1.48 | 1.37 | 1.46 | 1.36 | 1.93 |
| D2 | 2.39 | 2.42 | 1.51 | 1.50 | 1.35 | 1.50 | 1.37 | 1.98 |
| D3 | 2.34 | 2.42 | 1.36 | 1.50 | 1.57 | 1.60 | 1.53 | 1.98 |
| TwB | 2.35 | 2.35 | 1.36 | 1.48 | 1.57 | 1.57 | 1.57 | 1.96 |
| DB1 | 2.35 | 2.34 | 1.50 | 1.36 | 1.50 | 1.49 | 1.37 | 2.02 |
| TiB1 | 2.34 | 2.37 | 1.36 | 1.50 | 1.57 | 1.57 | 1.57 | 2.00 |

[a] All the C−C bonds reported are relative to the carbon Ring. Only the distances for the Si dimers bonded to the toluene molecule are reported. $C_b$ denotes a carbon atom bonded to a Si dimer. In the case of the $C_b$−Si bonds we have reported the average value.

presence of one C−C double bond in the ring. In these configurations the energy gained by the formation of four C−Si bonds between the C ring and the Si surface balances the loss of aromaticity of the ring. As a general behavior we find that the most stable undissociated configuration is obtained when the methyl group is as far away from the surface as possible, because of its steric hindrance. All the TiB configurations have only one C−C double bond formed by two $sp^2$-hybridized C atoms of the ring and four $sp^3$-hybridized C atoms bonded to the Si dimers of the surface, and differ only in the position of the methyl group. In the TiB1 configuration the double bond is located in the higher part of the backbone, close to the $CH_3$ group. This structure (shown in Figure 1) is particularly stable, because of the electron-donating effect of the methyl group to the C ring. The TiB3 configuration is less stable than TiB1 because the $CH_3$ is bonded to the C atom located in the opposite position with respect to the C−C double bond. The TiB2 structure has instead the $CH_3$ group bonded to a carbon atom adjacent to the double bond, with a binding energy intermediate between that of TiB1 and TiB3, as can be seen in Table 2. The TwB configuration is similar to the TiB one, being rotated by 90° with respect to the Si surface, and is slightly higher in energy than TiB.

Our calculations show that there are, with somewhat lower binding energies, three different, stable chemisorbed structures, characterized by only two C−Si bonds (SB, T, and DB; see Figure 1) and two C−C double bonds within the ring. Given the reduced number of C−Si bonds with the surface, which do not balance the loss of aromaticity of the molecule, for these configurations a lower binding energy is expected with respect to the TiB and TwB structures described above.

In the "standard butterfly" (SB) configuration the toluene molecule is bonded to a single surface Si dimer, and is characterized by two C−C double bonds on each "wing" of the butterfly. The SB1 configuration (with the $CH_3$ group bonded to a C atom involved in a double bond; see Figure 1) is more stable than SB2, where the $CH_3$ group is bonded to a C atom, forming a C−Si bond (see Table 2), because the methyl group has no steric hindrance and is bonded to an $sp^2$-hybridized C atom; actually the SB1 structure turns out to have a binding energy close to that of the TiB and TwB structures.

The "tilted" (T) configuration, shown in Figure 1, resembles the $\beta$ state proposed by Li and Leung[14] as a possible adsorption configuration of the intact toluene molecule. The different binding energies of the T1, T2, and T3 structures are reported in Table 2. Among the T configurations those with the methyl group in position 2 or 3 are energetically less favored than that with $CH_3$ in position 1. As can be seen our calculations show that these structures are the least stable among those investigated.

The "diagonal bridge" (DB) structure (see Figure 1) bridges two adjacent surface dimers. Ab initio MD simulations indicate that the process of chemisorption into the DB structure is barrierless (the toluene molecule, initially placed close to the Si(100) surface, spontaneously sticks to the surface). This result, together with a preliminary analysis of theoretical STM images,[31] suggests that the DB structure could be the metastable state conjectured by some authors, and which has been associated with the "M" structure observed in STM experiments.[13] In fact our computed STM image of the DB structure shows some similarities with the STM experimental image of the M state, being characterized by a bright spot that involves the two Si dimers to which the toluene molecule is attached; note that, in the DB configuration, the Si dimers remain buckled (the buckling is stabilized), while, for instance, in the SB structure the Si dimer on which the toluene molecule is bonded becomes essentially flat (the buckling is hindered). All other configurations of the intact molecule shown in Figure 1 are apparently characterized by a finite energy barrier opposing their attachment to the Si surface. Thus, their physical realization needs the presence of some kind of precursor states, where the intact molecule is weakly bound to the surface by van der Waals interactions. We cannot guess what these precursor states are, nor can we estimate the energy barriers separating these physisorbed states from the chemisorbed configurations shown in Figure 1 because of the lack of long-range dispersion forces in our DFT approach.

Li and Leung[14] proposed, as a stable adsorbed configuration in which the toluene molecule forms four C−Si bonds with two surface Si dimers, a "pedestal" (P) one (the $\gamma$ state shown in Table 1 of ref 14); however, similarly to the case of benzene on Si(100),[11] according to our calculations this configuration is actually found to be unstable.

In general, we observe that toluene binds to the Si(100) surface more strongly than benzene, as can be seen comparing the binding energies of two representative configurations, SB and TiB: in both the cases the binding energy of toluene is found to be higher by about 0.3 eV than that of benzene. This theoretical result confirms the analysis of recent experimental measurements.[14]

Considering now the possible *dissociated* structures, we found two configurations, D1 and D2 (see Figure 2), whose binding energies are larger than those of all the undissociated structures discussed above, and which occur after hydrogen abstraction from the methyl group; this process favors in turn the $\sigma$ bonding of the remaining methylene ($CH_2$) group to the Si surface. Note that breaking of a C−H bond in the methyl group is expected to be favored with respect to breaking of a C−H bond in the aromatic ring; in fact, in the case of the free toluene molecule, this process requires 3.69 eV to be compared to the energy of

4.77 eV required to break a C−H bond in the aromatic ring.[30] Our D1 structure corresponds to the configuration $\beta$ proposed by Li and Leung (see Table 1 in ref 14) as a candidate for the dissociated state of toluene on Si(100), and could be obtained starting from the undissociated chemisorbed structure T1 discussed previously. According to our results, however, it appears that a good candidate for the $\beta$ structure is more likely the D2 configuration (which can be obtained starting from the undissociated SB1 configuration), since it is more stable than the D1 one (see Table 2); moreover, it originates from a configuration of the intact molecule (SB1) which is also energetically favored with respect to the one (the T structure) from which the D1 structure can be obtained. Actually the experimental occurrence of a given dissociation reaction is largely determined by kinetic effects; i.e., one should consider the overall reaction pathways connecting the undissociated configuration to the dissociated products. We will address this important issue in the following.

We have also considered another possible dissociated configuration, D3, characterized by the abstraction of the whole methyl group from the carbon ring, with subsequent sticking of this fragment to a Si atom of a clean surface dimer (see Figure 2). This structure extends over three adjacent Si surface dimers. Therefore, it can be properly described only using our larger supercell: in the smaller one, due to spurious interactions of the structure with its periodically repeated images, this configuration is found to be unstable. It appears from Table 2 that the D3 structure is energetically less favored than the D1 and D2 configurations.

In Table 2 we compare our calculated binding energies obtained using the two different supercells; note that the larger supercell corresponds to a lower coverage (one toluene molecule per eight surface Si dimers) than that realized with the smaller one (one toluene molecule per four surface Si dimers). As can be seen, the energetic ordering is not substantially altered when the larger supercell is used (with the exception of the relative stability of the TwB and SB1 structures), although binding energies relative to the larger supercell are systematically larger. In both cases the D2 structure is by far the most stable one among those investigated. The observed differences in the binding energies discussed above can be mainly attributed to the different coverages and the consequent different adsorbate−adsorbate interactions, which, from the results reported in the table, appear to be repulsive for the structures which have been investigated with both supercells.

In Table 3 we report the structural parameters relative to the different adsorption configurations studied. Average bond lengths for the double and the single C−C bonds are 1.36 and 1.51 Å , respectively. Note that the lengths of the C−C bonds involving C atoms of the ring bonded to the Si surface are longer, some of them being close to 1.6 Å.

We will address next the important problem of determining the reaction paths, together with their associated energy barriers, leading from a stable adsorption structure of the intact toluene molecule to the dissociated configurations, D1, D2, and D3. The reaction pathways have been determined from first principles, as described in the Method, by using the CI-NEB method.[29] We summarize in Table 4 our calculated values for the energy barriers for the various reactions considered here.

In Figure 3 we show the MEP for the transformation going from the SB1 structure to the D2 structure (the most stable one): as can be seen the energy barrier relative to this pathway is about 1.4 eV. Instead the path for the transition from the T1 configuration to the D1 configuration is characterized by an

**TABLE 4: Energy Barriers (eV) for the Minimum Energy Paths Studied from First Principles**[a]

| reaction path | energy barrier | reaction path | energy barrier | reaction path | energy barrier |
|---|---|---|---|---|---|
| SB1−D2 | 1.4 | T2−TiB2 | 0.5 | DB1−TiB2 | 0.8 |
| T1−D1 | 1.5 | SB1−TiB1 | 0.9 | TiB1−D3 | 3.2 |

[a] For the TiB1−D3 reaction path the larger $p(4\times4)$ supercell has been used, while, in all the other cases, the $p(\sqrt{8}\times\sqrt{8})R45°$ supercell has been used.

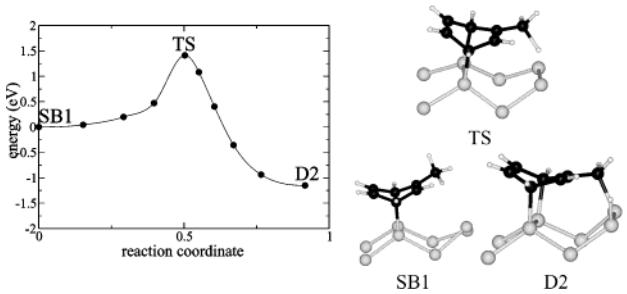


**Figure 3.** Dissociative reaction path for the transformation going from the SB1 structure to the D2 structure. TS denotes the transition state.

energy barrier of 1.5 eV (such a process has been suggested by Li and Leung[14]). In both these dissociation processes the detached H atom bonds to the "up" Si atom (the nucleophilic one) of a neighbor surface dimer, the breaking of a C−H bond of the methyl group being more than offset by the formation of two new bonds, a H−Si bond and a C−Si bond. A rough estimate of the reaction rate $k$ for these dissociative reactions can be obtained by using the Arrhenius formula[32] (i.e., assuming first-order kinetics): $k = Ae^{-Ea/K_BT}$, where $E_a$ is the energy barrier for the reaction, $T$ is a typical experimental temperature[14] (430 K), and the prefactor $A$ can be estimated to be in the range[33] $10^{13}-10^{15}$ s$^{-1}$; we obtain, in the case of the MEP leading from the SB1 structure to the D2 structure, $4 \times 10^{-4}$ s$^{-1}$ < $k$ < $4 \times 10^{-2}$ s$^{-1}$, while for the MEP from the T1 structure to the D1 structure we obtain $3 \times 10^{-5}$ s$^{-1}$ < $k$ < $3 \times 10^{-3}$ s$^{-1}$. To better characterize the SB1−D2 transformation, we have also generated, for each step of the reaction path, the maximally localized Wannier functions,[34] which allow the total charge to be partitioned in a chemically transparent and unambiguous way. Interestingly, looking at the trajectories of the Wannier function centers, it is evident that the valence electron of the H atom detached from the methyl group does not follow the proton but contributes to the formation of a new C−Si bond, so the reaction can be described in terms of a proton abstraction (or proton transfer) process in which the proton forms a new bond with the nucleophilic, up Si atom of the dimer by exploiting the excess negative charge localized on this atom. This result is also confirmed by the fact that spin-restricted and -unrestricted calculations give results that are very similar (in terms of the location of the Wannier function centers and the shape of the Wannier functions), thus suggesting that the process can be well described in terms of paired electrons. Probably a similar scenario applies also to the case of the T1−D1 transformation. As far as a possible pathway leading to the D3 configuration is concerned, we only found an MEP, starting from the TiB1 structure, characterized by a very high (about 3.2 eV) energy barrier, which makes this dissociation reaction very unfavored.

We have also considered transitions in which the molecule goes from a chemisorption configuration characterized by two C−Si bonds to one with four C−Si bonds. In particular, the MEP from the T2 structure to the TiB2 one has an energy barrier of 0.5 eV, while that from SB1 to TiB1 has an energy barrier

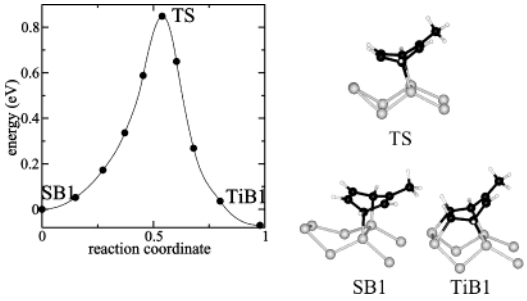


**Figure 4.** Reaction path for the transformation going from the SB1 structure to the TiB1 structure.

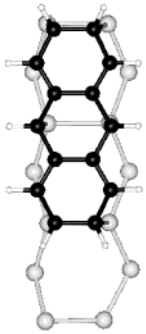

**Figure 5.** Polymerized chemisorbed structure obtained by joining two toluene molecules on the Si(100) surface (see the text for details).

of 0.9 eV (see Figure 4); the corresponding reaction rates are estimated to be (at 430 K) $1.4 \times 10^7\ s^{-1} < k < 1.4 \times 10^9\ s^{-1}$ and $3 \times 10^2 < k < 3 \times 10^4\ s^{-1}$, respectively. The SB1−TiB1 transition, which has a relatively low energy barrier, is probably favored by the attraction between the double-bond charge of the "wing" of the SB1 structure and the down (electrophilic) Si atom of a surface dimer. We can see this reaction like a classic addiction reaction, as explained in the Introduction, in which the electrophilic moiety (in this case the down Si atom of a surface dimer) attacks the carbon involved in the double bond. Similar considerations apply also to the T2−TiB2 transition. Finally, we have found a possible transition going from the DB1 structure (which could be the metastable state observed in STM experiments[13]) to the TiB2 one: this process, which requires the breaking of a C−Si bond and the formation of three new C−Si bonds, has an energy barrier of 0.8 eV.

Interestingly, Li and Leung[14] have conjectured that thermal decomposition of adsorbed toluene in the 750−950 K range may result in the formation of complex molecular structures characterized by three connected phenyl rings, through the reaction of *two* toluene molecules at the Si(100) surface. We have studied the possibility of such a reaction by looking at a configuration (shown in Figure 5) which can be obtained by joining two toluene molecules (due to the spatial dimensions of the resulting structure, the larger supercell has been used to avoid finite-size effects). To make possible the realization of the structure proposed in ref 14 starting from two toluene molecules, six H atoms must be detached from the rings and bind to nonsaturated surface Si dimers. The gain in energy in realizing this structure is substantial, since its binding energy (5.72 eV) is much larger than the sum of the binding energies of two noninteracting toluene molecules in the D1 configuration (see Table 2). Although it is not easy to estimate the energy barriers that the system should overcome to produce such a polymerized chemisorbed structure, this result seems to confirm the conjecture of Li and Leung and suggests that it could be worthwhile to study similar condensation reactions using toluene or other organic molecules containing more than one methyl group. We are currently investigating these processes.[35]

## IV. Conclusions

Ab initio simulations, supplemented by semiempirical potential calculations, have been used to investigate the chemisorption of toluene on the Si(100) surface. Different chemisorption configurations are possible, for which we have computed structural and energetical properties. We confirm that toluene, in contrast with the case of benzene on Si(100), can dissociate upon adsorption and that the favored dissociation path involves the cleavage of C−H bonds of the methyl group. Several other possible reaction pathways have been investigated. A possible metastable state has been identified, which could be that suggested in ref 13.

**Acknowledgment.** We acknowledge financial support from INFM, through the PRA "1MESS", and allocation of computer resources from INFM "Progetto Calcolo Parallelo".

## References and Notes

(1) Arthur, J. *Surf. Sci.* **2002**, *500*, 189.

(2) Weldon, M. K.; Queeney, K. T.; Eng, J., Jr.; Raghavachari, K.; Chabal, Y. J. *Surf. Sci.* **2002**, *500*, 859.

(3) Yates, J. T., Jr. *Science* **1998**, *279*, 335.

(4) Hovis, J. S.; Hamers, R. J. *J. Phys. Chem. B* **1997**, *101*, 9581.

(5) Masri, P. *Surf. Sci. Rep.* **2002**, *48*, 1.

(6) Taguchi, Y.; Fujisawa, M.; Takaoka, T.; Okada, T.; Nishijima, M. *J. Chem. Phys.* **1991**, *95*, 6870.

(7) Lopinski, G. P.; Fortier, T. M.; Moffatt, D. J.; Wolkow, R. A. *J. Vac. Sci. Technol., A* **1998**, *16*, 1037.

(8) Lopinski, G. P.; Moffatt, D. J.; Wolkow, R. A. *Chem. Phys. Lett.* **1998**, *282*, 305. Borovsky, B.; Krueger, M.; Ganz, E. *Phys. Rev. B* **1998**, *57*, R4269.

(9) Wolkow, R. A.; Lopinski, G. P.; Mofatt, D. J. *Surf. Sci.* **1998**, *416*, L1107.

(10) Kong, M. J.; Teplyakov, A. V.; Lyubovitsky, J. G.; Bent, S. F. *Surf. Sci.* **1998**, *411*, 286.

(11) Silvestrelli, P. L.; Ancilotto, F.; Toigo, F. *Phys. Rev. B* **2000**, *62*, 1596.

(12) Coulter, S. K.; Hovis, J. S.; Ellison M. D.; Hamers R. J. *J. Vac. Sci. Technol., A* **2000**, *18*, 1965.

(13) Borovsky, B.; Krueger, M.; Ganz, E. *J. Vac. Sci. Technol., B* **1999** *17*, 7.

(14) Li, Q.; Leung, K. T. *Surf. Sci.* **2001**, *479*, 69.

(15) Car, R.; Parrinello, M. *Phys. Rev. Lett.* **1985**, *55*, 2471. We have used the code CPMD, version 3.5, developed by J. Hutter et al. at the MPI für Festkörperforschung and IBM Research Laboratory (1990−2001).

(16) Perdew, J. P.; Burke, K.; Ernzerhof, M. *Phys. Rev. Lett.* **1996**, *77*, 3865.

(17) Sorescu, D. C.; Jordan, K. D. *J. Phys. Chem. B* **2000**, *104*, 8259.

(18) Nachtigall, P.; Jordan, K. D.; Smith, A.; Jonsson, H. *J. Chem. Phys.* **1996**, *104*, 148.

(19) Troullier, N.; Martins, J. *Phys. Rev. B* **1991**, *43*, 1993.

(20) Silvestrelli, P. L.; Toigo, F.; Ancilotto, F. *J. Chem. Phys.* **2001**, *114*, 8539.

(21) Silvestrelli, P. L.; Sbraccia, C.; Ancilotto, F. *J. Chem. Phys.* **2002**, *116*, 6291.

(22) Shkrebtii, A. I.; Di Felice, R.; Bertoni, C. M.; Del Sole R. *Phys. Rev. B* **1995**, *51*, 11201. Gay, S. C.; Srivastava, G. P. *Phys. Rev. B* **1999**, *60*, 1488 and references therein.

(23) Hutter, J.; Luthi, H. P.; Parrinello, M. *Comput. Mater. Sci.* **1994**, *2*, 244.

(24) Abell G. C. *Phys. Rev. B* **1985**, *31*, 6184.

(25) Brenner, D. W. *Phys. Rev. B* **1990**, *42*, 9458.

(26) Dyson, A. J.; Smith, P. V. *Surf. Sci.* **1996**, *355*, 140; **1997**, *375*, 45.

(27) Que, J.-Z.; Radny, M. W.; Smith, P. V. *Phys. Rev. B* **1999**, *60*, 8686.

(28) Sbraccia, C.; Silvestrelli, P. L.; Ancilotto, F. *Surf. Sci.* **2002**, *516*, 147.

(29) Henkelman, G.; Uberuaga, B. P.; Jónsson, H. *J. Chem. Phys.* **2000**, *113*, 9901. Henkelman, G.; Jónsson, H. *J. Chem. Phys.* **2000**, *113*, 9978.

(30) Weast, R. C.; Ed. *CRC Handbook of Chemistry and Physics*, 64th ed.; CRC Press Inc.: Boca Raton, FL, 1983.

(31) We have generated "theoretical" STM images, using the simplest approximation based on the Tersoff−Hamann theory; see: Tersoff, J.; Hamann, D. R. *Phys. Rev. Lett.* **1983**, *50*, 1998.

(32) Of course the Arrhenius estimate of the rate constant is very rough and can be off even by some orders of magnitude. In principle more sophisticated and more accurate approaches exist; see, for instance: Dellago, C.; Bolhuis, P. G.; Chandler, D. *J. Chem. Phys.* **1999**, *110*, 6617.

(33) Smith, A. P.; Jónsson, H. *Phys. Rev. Lett.* **1996**, *77*, 1326.

(34) Marzari, N.; Vanderbilt, D. *Phys. Rev. B* **1997**, *56*, 12847. Silvestrelli, P. L.; Marzari, N.; Vanderbilt, D.; Parrinello, M. *Solid State Commun.* **1998**, *107*, 7.

(35) Costanzo, F.; Silvestrelli, P. L.; Ancilotto, F. Unpublished results.